Bioorganic & Medicinal Chemistry 19 (2011) 1606–1612

Contents lists available at ScienceDirect

Bioorganic & Medicinal Chemistry

journal homepage: www.elsevier.com/locate/bmc

X-ray and molecular modelling in fragment-based design of three small quinoline scaffolds for HIV integrase inhibitors

Katarzyna Majerz-Maniecka [a,*], Robert Musiol [b,*], Agnieszka Skórska-Stania [a], Dominik Tabak [b], Pawel Mazur [b], Barbara J. Oleksyn [a], Jaroslaw Polanski [b]

[a] Faculty of Chemistry, Jagiellonian University, ul. R. Ingardena 3, 30-060 Kraków, Poland
[b] Institute of Chemistry, University of Silesia, ul. Szkolna 9, 40-007 Katowice, Poland

ARTICLE INFO

Article history:
Received 23 November 2010
Revised 20 January 2011
Accepted 21 January 2011
Available online 27 January 2011

Keywords:
HIV integrase
Quinolines
Fragment-based drug design
Crystal structure

ABSTRACT

Crystal structures of three small molecular scaffolds based on quinoline, 2-methylquinoline-5,8-dione, 5-hydroxy-quinaldine-6-carboxylic acid and 8-hydroxy-quinaldine-7-carboxylic acid, were characterised. 5-Hydroxy-quinaldine-6-carboxylic acid was co-crystallized with cobalt(II) chloride to form a model of divalent metal cation–ligand interactions for potential HIV integrase inhibitors. Molecular docking into active site of HIV IN was also performed on 1WKN PDB file. Selected ligand–protein interactions have been found specific for active compounds. Studied structures can be used as scaffolds in fragment-based design of new potent drugs.

1. Introduction

Recently the fragment-based approach (F-BA) to drug discovery has gained stronger attention than ever before. During the last 10 years this methodology has been intensively developing and now it can be successfully used as an alternative for poorly effective HTS.[1,2] However, it should be remembered that the molecules used as fragments do not possess high activity, but they are much more druggable than huge, sophisticated structures usually pointed out in HTS. Thus, in F-BA we are looking rather for possibility of creating a new drug than for activity. Successful molecular scaffolds should be easily accessible and transferable into real drug. Probably the best way to achieve this aim is to explore the so-called privileged structures as a scaffold.[3] Unfortunately there are no simple rules that specify which structure is really privileged. On the other hand quinoline and its derivatives such as quinolone antibiotics can be the most spectacular examples of the potential efficiency of this system.[4] Quinine molecule, which also contains a quinoline moiety, proves the Nature preference for this system. Quinoline scaffold can also be found in many classes of other biologically active compounds used as antifungals, antibacterials and antiprotozoic drugs[5–8] as well as antituberculotic agents.[9] Some quinoline analogues showed also antineoplastic activity. Thorough knowledge of all interactions which occur in solutions or crystals of molecules proposed as scaffolds is very important for better understanding its fate in biological systems and for (Q)SAR studies. Certain specific interactions are able to change crucial parameters of molecules or even to change the structure via shift of tautomeric equilibrium.[10] Here we wish to report our findings concerning intermolecular interactions in the crystal structures of three quinoline-based scaffolds that are promising in design of new antiviral and anticancer agents (Fig. 1). In the next stage, we applied molecular docking to correlate data derived from crystal structure and biological activity.

Quinoline-5,8-dione is a substantial molecular fragment of lavendomycin and related compounds (Fig. 2). Lavendomycin was originally isolated from the fermented broth of *Streptomyces lavendulae* and the compounds of this class were identified in the 1970's as anti-tumour agents. Although the toxicity of lavendomycin makes it unsuitable for clinical use, its activity has inspired several investigations.[11–14] This scaffold was found to be very

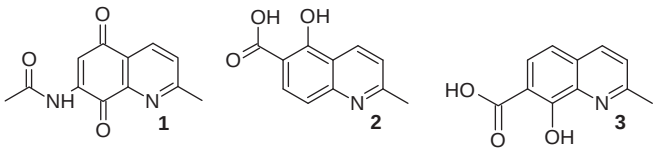

Figure 1. Three molecular scaffolds as fragments of HIV integrase inhibitors.

* Corresponding authors.
E-mail addresses: majerz.maniecka@gmail.com (K. Majerz-Maniecka), robert.musiol@us.edu.pl (R. Musiol).

0968-0896/$ - see front matter © 2011 Elsevier Ltd. All rights reserved.
doi:10.1016/j.bmc.2011.01.045

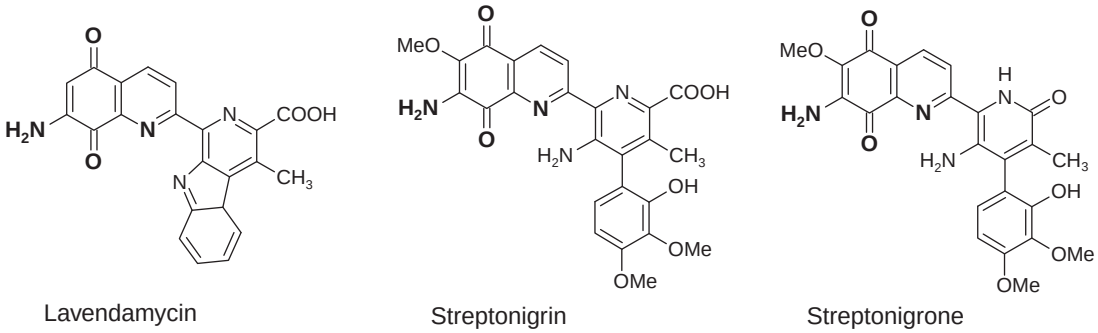

Figure 2. Quinolinone-based antibiotics show the importance of quinoline as molecular fragment.

promising in our recent investigation of anticancer agents with activity against P-388 leukaemia cells twice as high as that of cisplatin.[15]

5-Hydroxy-quinaldine-6-carboxylic acid (Fig. 1(2)) proved its applicability in design of novel HIV integrase inhibitors[16,17] and herbicidal agents.[18] Its isomer, 8-hydroxy-quinalidne-7-carboxylic acid, is a well-known scaffold used in synthesis of potent HIV integrase inhibitors (e.g., FZ41), antifungal and anticancer agents.[19–22]

Most of HIV integrase inhibitors are believed to interact with divalent metal cations such as magnesium or manganese, located at the protein active site.[23] Recently retroviral intasome has been elucidated by mean crystal structure of IN from PFV virus.[24,25] This can also confirmed importance of this mechanism. Elvitegravir and raltegravir two known potent inhibitors of HIV integrase were found engaging two Mg cations in the active site of the intasome.[26] It seems obvious that knowledge of interactions between an inhibitor molecule and cations is crucial for better understanding its mode of action and explaining its activity and/or selectivity.[27] Furthermore they can also be useful in elucidation the problem of drug resistance caused by small mutations.[28]

2. Results and discussion

2.1. Chemistry

Synthesis of studied scaffolds is depicted in Scheme 1.

Compound **1** was obtained from 2-methyl-8-hydroxyquinoline through nitration, reduction and finally oxidation to give crude product (purified by crystallization from EtOH) as yellow solid, 80% yield, mp 258 °C (lit. mp 260.5 °C[29]). Compound **2** was obtained from 2-hydroxy-4-aminobenzoic acid and crotonaldehyde in Skraup reaction.[16] 8-Hydroxy-2-methylquinoline-7-carboxylic acid **3** was obtained in Kolbe–Schmidt reaction from 8-hydroxyquinaldine as described earlier.[21]

2.2. Crystal structures

Single crystals of compound **1** (CCDC 752663) were obtained from ethanol solution, while compound **2** (CCDC 752665) was co-crystallized with cobalt dichloride hexahydrate also from ethanol. Single crystals of compound **3** (CCDC 795948) developed in dimethyl sulfoxide and ethanol solution (1 v/1 v). All the crystals were grown by slow evaporation of the solvent, at a temperature of about 293 K. X-ray data were collected on a Bruker-Nonius KappaCCD diffractometer using MoKα radiation. The phase problem was solved by direct methods using SIR[30] and refined by full matrix least-squares method using SHELX97.[31] Hydrogen atoms were located in difference Fourier maps and refined isotropically, using riding model.

The details of the crystal data, data collection and refinement are listed in Table 1, while the asymmetric units of these structures together with atom numbering are shown in Figure 3. All projections were generated using ORTEP.[32]

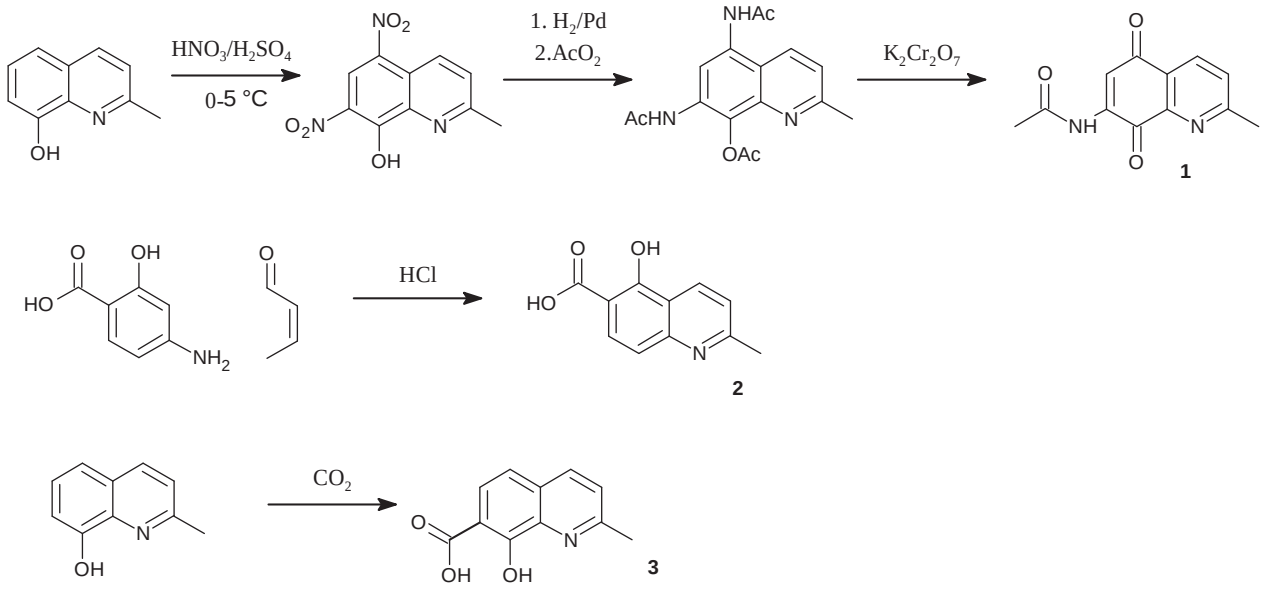

Scheme 1. Synthesis of quinolines **1**–**3**.

Table 1
Crystal data, measurement and calculation details

Chemical formula	Structure **1** $C_{12}H_{10}N_2O_3$	Structure **2** $2[C_{11}H_8NO_3{\cdot}HCl]^-{\cdot}[Co(H_2O)_4]^{2+}$	Structure **3** $[C_{11}H_{10}NO_3]^+{\cdot}Cl^-$
Crystal data			
M (g mol^{-1})	230.339	304.14	239.759
Crystal system	Triclinic	Triclinic	Triclinic
Space group	$P\bar{1}$	$P\bar{1}$	$P\bar{1}$
a [Å]	3.864(3)	7.274(3)	7.207(1)
b [Å]	11.545(1)	7.413(3)	9.470(2)
c [Å]	14.049(1)	11.874(6)	9.639(2)
α [°]	104.33(3)	91.38(2)	97.21(1)
β [°]	94.16(2)	103.40(2)	109.52(1)
γ [°]	92.45(5)	94.75(2)	108.12(1)
V [Å^3]	604.43(9)	620.10(5)	569.64(2)
Z	2	2	2
D [g cm^{-3}]	1.265	1.629	1.502
F (0 0 0)	240	313	268
μ [mm^{-1}]	0.093	0.968	0.338
Data collection			
h_{min}, h_{max}	−5, 5	−9, 9	−9, 9
k_{min}, k_{max}	−15, 15	−9, 9	−12, 12
l_{min}, l_{max}	−15, 18	−15, 15	−12, 12
Θ range [°]	3.58–27.67	2.76–27.51	1.00–27.48
Unique reflns	3665	4855	5054
Reflns $F_0 > 4\delta(F_0)$	2667	2825	2615
Refinement			
R_1 for $F_0 > 2\delta(F_0)$	0.0847	0.0605	0.0376
R_1 for all data	0.1790	0.0893	0.0462
wR_2 for $F_0 > 2\delta(F_0)$	0.2539	0.1324	0.1084
GOOF on F^2	1.032	1.020	1.059

2.2.1. Molecule 1

The asymmetric unit of **1** consists of one molecule (Fig. 3(1)). The bond lengths C7–C8 and C5–C10 are 1.354(5) Å and 1.377(5) Å, respectively, and they are shorter than typical C_{Ar}–C_{Ar} distances.[33] The C6–O1 and C9–O2 bonds demonstrate double character, which suggest electron localisation of quinolinedione arrangement of the ring. The valence angles C5–C6–C7 = 118.4(3)° and C8–C9–C10 = 118.5(3)° are smaller than 120°, which can be ascribed, according to VSEPR theory, to the influence of oxygen free electron pairs and C–O double bonds. The high values of the atomic displacement parameters for the methyl group and for oxygen can be explained by the rotational freedom (O3) and certain possibility of disorder (O1, O2). The ring system of the molecule **1** is almost planar and coplanar with the substituents, the greatest distortion, 0.107(5) Å, being that of the O3 atom. Also torsion angles, C10–C5–C6–O1 = 177.8(4)°, C7–C8–C9–O2 = −179.6(4)°, C7–C8–N2–C11 = −3.3(7)°, C8–N2–C11–O3 = −1.2(7)°, C8–N2–C11–C12 = −179.6(4)°, confirm planarity of the whole molecule. The packing of the molecules in the unit cell is dominated mainly by hydrogen bonds and π–π interactions. The details of hydrogen bond geometry are given in Table 2. The proton of N2 atom is shared by two oxygen atoms with formation of a bifurcated hydrogen bond. The intermolecular contact N2–H2···O2 represents rather a weak hydrogen bond interaction as shown by the donor–acceptor distance (Table 2).

This situation is most probably caused by the steric hindrance introduced by methyl groups. Intramolecular N2–H2···O2 hydrogen bond is another example of weak interaction because it leads to formation of a strained pentagonal ring. There are also π–π interactions in structure of **1** as shown by the distance between centroids of neighbouring rings, which is 3.864(3) Å. This distance is equal to the unit cell parameter a, which shows that the 'sheets' of molecules **1,** parallel to (1 0 0) planes, are densely stacked in the crystal.

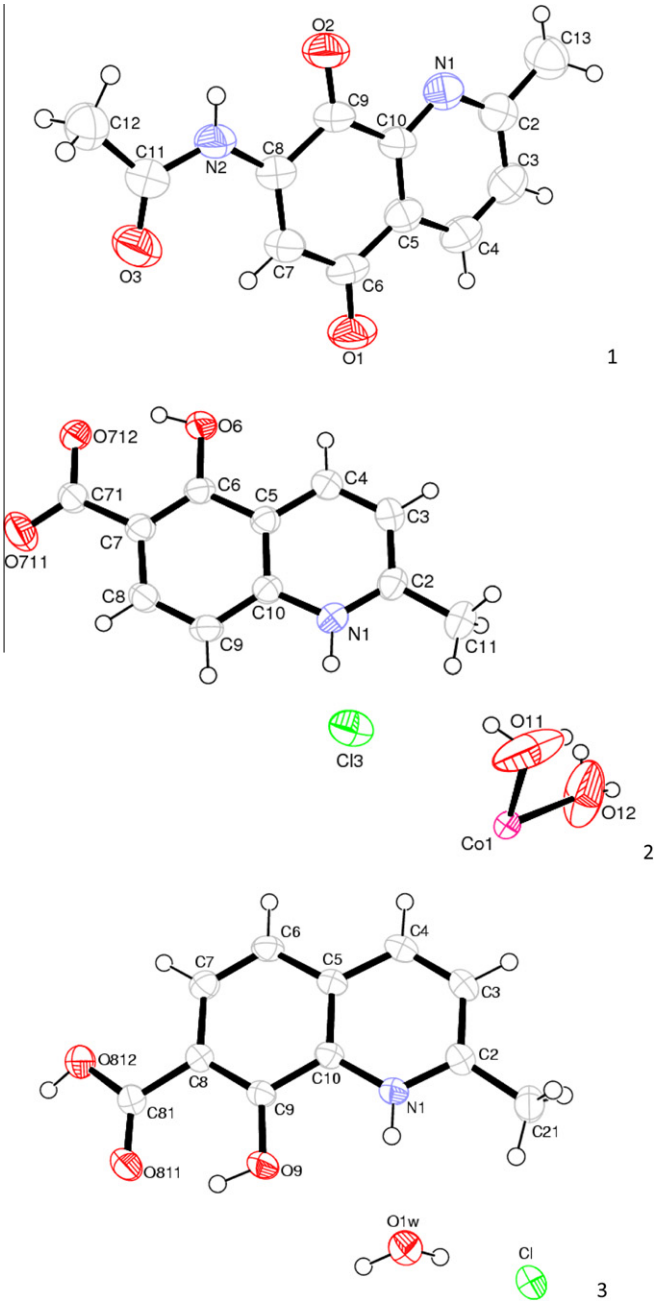

Figure 3. ORTEP projection of the asymmetric units of structures **1**–**3**.

Table 2
Hydrogen bonds geometry in the crystal structure of **1**

D–H	A	d(D–H) [Å]	d(H···A) [Å]	∠ DHA [°]	d(D···A) [Å]
N2–H2	O2i	0.83(4)	2.33(4)	176(3)	3.15(4)
N2–H2	O2	0.83(4)	2.33(4)	102(3)	2.63(1)

Symmetry codes (i) $-x+3$, $-y$, $-z+1$.

2.2.2. Molecule 2

The asymmetric unit of **2** consists of one molecule **2,** protonated at N1, one chloride anion, the cobalt cation and two water molecules (Fig. 3(2)). Since the Co^{2+} position is that of the inversion centre (1/2, 1/2, 1/2), this ion is present at half-occupancy. Water molecules linked with the cobalt cation show the highest atomic displacement parameters because of their disorder.

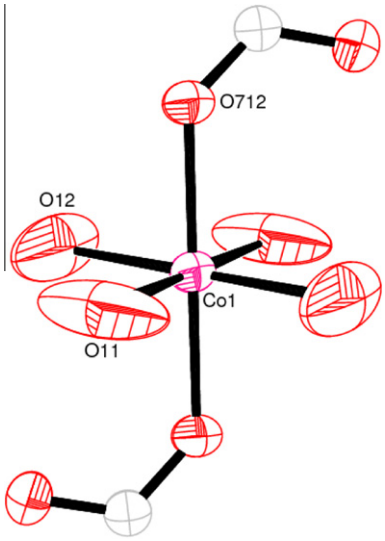

Figure 4. Cobalt cation environment.

Table 3
Hydrogen bonds geometry in the crystal structure of **2**

D–H	A	d(D–H) [Å]	d(H···A) [Å]	∠ DHA [°]	d(D···A) [Å]
O11–H111	O712i	0.88(2)	2.42(4)	113(3)	2.88(5)
O11–H111	O711i	0.88(2)	2.52(7)	120(6)	3.06(6)
O12–H121	O711i	0.91(2)	2.56(8)	133(9)	3.25(7)
O12–H122	O711ii	0.89(2)	2.11(6)	129(6)	2.75(6)
O11–H112	O12	0.89(2)	2.42(4)	118(3)	2.94(1)
N1–H1	Cl3	0.91(4)	2.21(4)	168(4)	3.11(4)
O6–H61	O712	0.87(5)	1.70(5)	151(5)	2.49(4)

i = $-x$, $-y$, $-z$; ii = x, $y+1$, $z+1$.

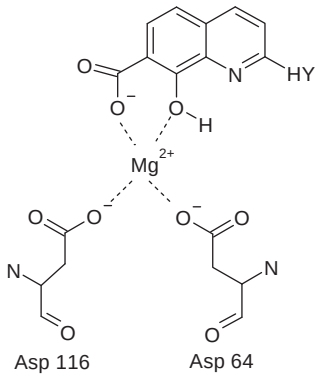

Figure 5. Hypothetical mechanism of quinoline derivative—magnesium cation interaction[35] at the active site of HIV integrase. HY-hydrophobic moiety.

The bond lengths, bond angles and torsion angles are comparable to those typical for similar compounds.[23]

The relatively high value of C2–N1–C10 angle, equal to 123.9(3)°, is most probably the result of N1 protonation.

The coordination sphere of the cobalt cation is occupied by the oxygen atoms belonging to four water molecules and two molecules **2** (Fig. 4).

The O–Co–O angles are approximately equal to 90°, which leads to octahedral environment of Co. Crystal structure of **2** is stabilized by seven hydrogen bonds. The details of their geometry are given in Table 3.

Intramolecular O6–H61···O712 hydrogen bond is a weak interaction because it is strained by its participation in the six-membered ring which consist of C6, O6, H61, O72, C71 and C7. Intermolecular O11–H111···O712i and O11–H11···1O711i interactions are bifurcated, and similar situation can be observed for

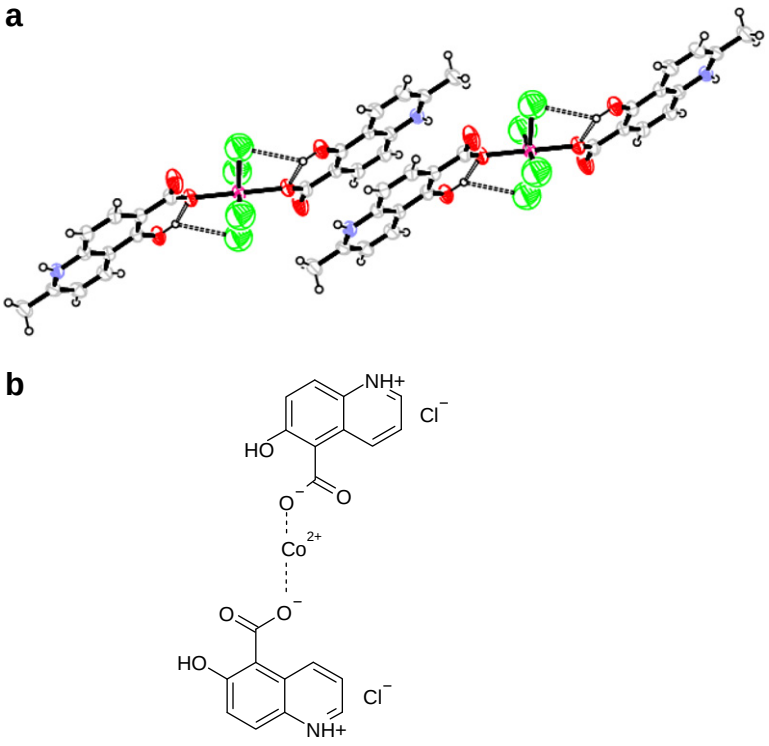

Figure 6. (a) Fragment of the crystal structure of **2** showing the coordination of Co cation and mutual π–π interactions between quinoline moieties of two complexes. (b) Scheme of cobalt cation interactions with carboxyl oxygen atoms.

Table 4
Hydrogen bonds geometry in the crystal structure of **3**

D–H	A	d(D–H) [Å]	d(H···A) [Å]	∠ DHA [°]	d(D···A) [Å]
N1–H1	O1 W	0.83(2)	2.01(2)	2.830(2)	166(2)
O9–H9	O811	0.89(2)	1.81(2)	2.590(2)	146(2)
O812–H812	Cli	0.87(2)	2.13(2)	2.965(1)	161(2)
O1W–H1W1	Cl	0.86(2)	2.31(2)	3.168(1)	177(2)
O1 W–H1W2	Clii	0.90(2)	2.39(2)	3.282(1)	170(2)

i = $x+1, y+1, z+1$; ii = $-x-1, -y+1, -z+2$.

O711i oxygen atom, which is an acceptor for two hydrogen atoms, H111 and H121. The strongest interaction is N1–H1···Cl3, where the chloride anion is the hydrogen acceptor.

Two molecules **2**, that coordinate cobalt cation, form a dimer, which is stabilized by the π–π interactions. The distance between centroids of quinoline ring is 4.00(3)Å.

Since the crystal structure of the salt $2[C_{11}H_8NO_3{\cdot}HCl]^{-}{\cdot}[Co(H_2O)_4]^{2+}$ is very interesting from the viewpoint of its inhibitory behaviour towards HIV integrase, it is described below in greater detail.

There are two hypotheses about magnesium cation—quinoline derivatives interactions at the active site of HIV integrase. According to the first of them one molecule of the inhibitor is in contact with two metal cations,[25–27,34] while according to the second hypothesis one quinoline interacts with one Mg cation.[23]

In the pattern shown in Figure 5 one molecule of inhibitor is in contact with magnesium cation via carboxyl and hydroxyl group, in position 7 and 8 of the quinoline ring, respectively. There are also two aspartic acid moieties (Asp 64 and Asp 116) and two water molecules in the octahedral Mg cation environment.

The model of interactions between the metal atom at the integrase active site and the quinoline inhibitor, which we can deduce from the Co-model inhibitor interactions in the crystal structure of molecule **2** (Fig. 6) is different.

The cobalt cation interacts with the oxygen atoms, which belong to the deprotonated carboxyl groups of two quinoline moieties, with Co–O distance equal 2.072(3) Å. The hydroxyl group is a proton donor in the intramolecular hydrogen bond, which stabilizes the orientation of substituents coplanar with the quinoline plane. It is interesting that, in spite of these differences, the Co–O distance is equal to those characteristic for Mg–O (2.073(2) Å) in magnesium–quinoline complex.[34] In this context we postulate that the cobalt cation might be a suitable model for prediction of the magnesium cation interactions with its environment.

2.2.3. Molecule 3

The asymmetric unit of the third structure contains one molecule **3**, in the hydrochloride form, and one water molecule (Fig. 3(3)). The bond lengths, bond angles and torsion angles are comparable to those typical for similar organic compounds.[33] The hydroxyl and methyl group are coplanar with the quinoline ring, the torsion angles C7–C8–C9–O9 and C4–C3–C2–C21 being −179.8(1)° and −178.5(1)°, respectively. The carboxyl group is deviated from planarity as shown by the C6–C7–C8–C81 angle value, −175.5(1)°. The packing of the molecules **3** in the crystal is dominated mainly by hydrogen bonds, see Table 4 for details. Intermolecular hydrogen bonds are formed between molecule **3** and water molecules, molecule **3** and the chloride anion and also between the water molecule and chloride anion. Intramolecular bond, O9–H9···O811, is weak because it leads to formation of strained hexagonal ring.

Crystal structure of **3** is also stabilized by π–π interactions between two quinolines, which are related via inversion centre. The distance between C10 atom of one molecule to the centroid of the neighbouring ring is 3.461(3) Å.

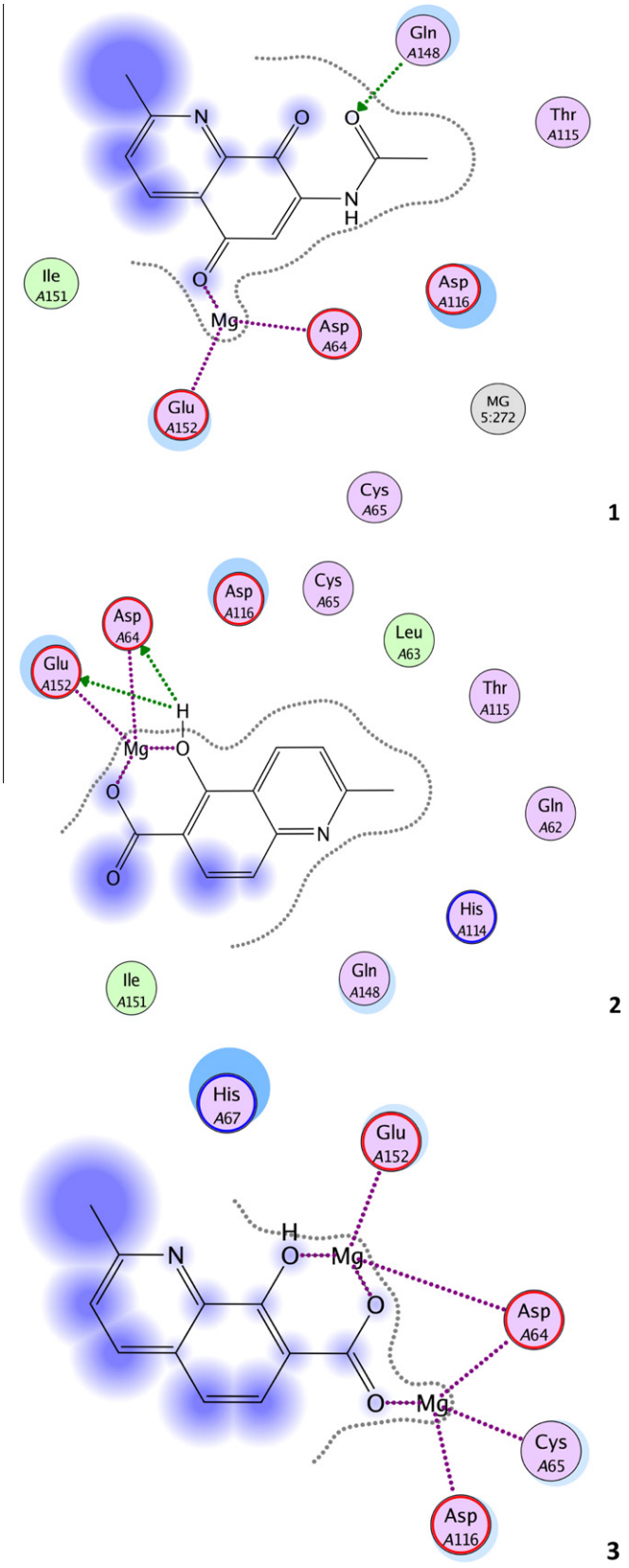

Figure 7. Compounds **1**–**3** docked into HIV IN active site.

2.3. Molecular docking simulations

Molecular modelling and molecular mechanics simulations were performed using the CCG MOE software packages running

Table 5
Selected interactions between studied compounds and HIV IN

Compound	IC_{50}[41] [μM]	LdG[a] [kcal/mol]	Interactions with Mg^{2+}	Interactions with aminoacids		
				Through Mg^{2+}	Hydrogen bonding	Indirect (allosteric)
1	77	−9, 67	O1–Mg	AspA64 GluA152	O3–GlnA148	AspA116
2	47[16]	−18, 75	O6–Mg–O711	AspA64 GluA152	O6H–AspA64 O6H–GluA152	AspA116
3	>100[21]	−14, 66	O9–Mg1–O812 O811–Mg	GluA152 AspA64 AspA116 CysA65	—	HisA67

[a] Calculated for the best docked pose of each structure.

on an Intel Pentium based machines with the GNU/Linux Debian operating system. Molecules **1**–**3** were collected in the input set and prepared for docking by standard procedure including the structure optimisation using the MMFF94x forcefield and calculation of the partial atomic charges using PM1 algorithm. Protomers and tautomers for these compounds were generated. Protein structure of HIV-1 integrase (full length DNA–integrase complex) was obtained from 1WKN PDB entry containing two aminoacid chains and two Mg^{2+} ions per each chain, bonded to ASP64, ASP116 and GLU152 residues. Additionally into the enzyme two strands of the viral DNA, segments: 1–25 and 26–52[36] has been docked. The integrase structure was prepared for docking by addition of missing hydrogen atoms, protein desolvatation, the calculation of the atomic partial charges (AMBER99 forcefield) and the protonation of the protein at physiological pH 7.4 using the PROPKA related method.[37] During docking a series of poses (ligand–protein complexes of particular conformation and mutual orientation) was generated for each molecule. The used alpha triangle docking algorithm consisted in alignment of triplets of ligand atoms on triplets of protein site points which are the centres of alpha spheres[38] created in the potential binding sites. During the simulation the poses were generated in sequence from a single conformer (protomer, tautomer) by applying a collection of preferred torsion angles to the rotatable bonds. The last stage of docking procedure was the energy minimisation and geometry optimisation of each docked pose in the binding site conditions. Classification of docking results was realized using London dG (LdG) scoring function (SF) which estimates the free energy of the ligand binding. A set of the highest scored poses were chosen for each molecule (pose) docked.[39]

According to some reports the scoring functions assessing molecular docking simulations should not be quantitatively correlated with activity.[40] Thus, in Figure 7 we present the two-dimensional ligand–receptor interaction diagrams which allows us to qualitatively observe binding in the presence of ligands.

This depicts relatively strong connections or hydrogen bonds as well as electrostatic or charge-transfer interactions between the ligand and the respective aminoacid residues. In Table 5 we have shown the interactions between ligand and protein in complex along with scoring functions and biological activities of the studied compounds. Activities are relatively low when compared to the leading structures described in literature. However, in case of fragment-based design this level of activity is quite promising for further optimisation. Nevertheless compound **3** can be regarded as inactive while **1** and **2** are moderately active. Further insight into the data collected in Table 5 provides some interesting remarks.

When compared only by scoring function, the scaffold **2** was docked at the active site with the lowest energy which can be ascribed to its high affinity, no doubt influencing the activity. Then 8-hydroxy-2-methylquinoline-7-carboxylic acid (**3**) seems to be favourably docked into the active site of HIV IN with strong interactions with two metal cations. On the other hand, it does not bind directly to aminoacids. Furthermore, the pattern of allosteric interactions in case of **1** and **2** is different from that observed in case of **3**. At the same time, compound **2** binds very efficiently and interacts with two aminoacids AspA64 and GluA152 by means of hydrogen bonding. Compound **1** binds relatively weakly to one Mg^{2+} cation and interacts with GlnA148. On this basis we can suggest different interactions pattern for structures **2** and its isomer **3**.

3. Conclusions

Three small molecular scaffolds used for fragment-based design of new HIV IN inhibitors were synthesized. Their crystal structures and in vitro activities were collected and molecular docking of studied compounds was performed. Some differences in the molecular interactions between inhibitors and enzyme seem to elucidate the activity pattern. Most active scaffold of 5-hydroxyquinaldine-6-carboxylic acid was found to be more efficient in hydrogen bonding interactions with enzyme active site than other two compounds. Further optimisation of this scaffold may lead to new interesting inhibitors.

Acknowledgements

This work was supported in part by KBN Grant PB1942/H03/2006/31 to K.M.-M. Molecular modelling was supported from PB N519 575638.

Supplementary data

Supplementary data associated with this article can be found, in the online version, at doi:10.1016/j.bmc.2011.01.045. These data include MOL files and InChiKeys of the most important compounds described in this article.

References and notes

1. Rees, D. C.; Congreve, M.; Murray, C. W.; Carr, R. *Nat. Rev. Drug Disc.* **2004**, *3*, 660.
2. Hajduk, P. J.; Greer, J. *Nat. Rev. Drug Disc.* **2007**, *6*, 211.
3. Kubinyi, H. Privileged Structures and Analogue-based Drug Discovery. In *Analogue-based Drug Discovery, IUPAC*; Fischer, J., Ganellin, C. R., Eds.; Wiley-VCH: Weinheim, 2006; pp 53–68.
4. Petersen, U. Quinolone Antibiotics: The Development of Moxifloxacin. In *Analogue Based Drug Discovery*; Fischer, J., Ganellin, C. R., Eds.; VCH-Wiley Verlag GmbH & Co., 2006; pp 315–370.
5. Fostel, J. M.; Lartey, P. A. *Drug Discovery Today* **2000**, *5*, 25.
6. Zainaba, D.; Meryem, L.; Abdelmejid, B.; Abdelfatah, A.; Mohammed, H.; Said, K.; Mohammed, B.; Mohammed, B. *Farmaco* **2004**, *59*, 195.
7. Musiol, R.; Serda, M.; Hensel-Bielowka, S.; Polanski, J. *Curr. Med. Chem.* **2010**, *17*, 1960.
8. Majerz-Maniecka, K.; Oleksyn, B.; Musiol, R.; Podeszwa, B.; Polanski, J. *Abstracts of Papers*, Joint Meeting on Medicinal Chemistry, Vienna, Austria, June 20–23, 2005. In Sci. Pharm. 2005; 73, 194.
9. Urbina, J.; Cortes, J.; Palma, A.; Lopez, S.; Kouznetsov, V. V.; Zacchino, S. A.; Enriz, R. D.; Ribas, J. C. *Bioorg. Med. Chem.* **2000**, *8*, 691.
10. Majerz-Maniecka, K.; Musiol, R.; Nitek, W.; Oleksyn, B. J.; Mouscadet, J.; Le Bret, M.; Polanski, J. *Bioorg. Med. Chem. Lett.* **2006**, *16*, 1005.

11. Doyle, T. W.; Balitz, D. M.; Grulich, R. E.; Nettleton, D. E.; Gould, S. J.; Tann, C.-H.; Meows, A. E. *Tetrahedron Lett.* **1981**, *22*, 4595.
12. Hackethal, C. A.; Golbey, R. B.; Tan, C. T. C.; Karnofsky, D. A.; Burchenal, J. H. *Antibiot. Chemother.* **1961**, *11*, 178.
13. Boger, D. L.; Mitscher, Y. M.; Drake, S. D.; Kitos, P. A.; Thompson, S. C. *J. Med. Chem.* **1987**, *30*, 1918.
14. Wilson, W. L.; Labra, C.; Barrist, E. *Antibiot. Chemother.* **1961**, *11*, 147.
15. Podeszwa, B.; Niedbala, H.; Polanski, J.; Musiol, R.; Tabak, D.; Finster, J.; Serafin, K.; Milczarek, M.; Wietrzyk, J.; Boryczka, S.; Mól, W.; Jampilek, J.; Dohnal, J.; Kalinowski, D. S.; Richardson, D. R. *Bioorg. Med. Chem. Lett.* **2007**, *17*, 6138.
16. Polanski, J.; Niedbala, H.; Musiol, R.; Podeszwa, B.; Tabak, D.; Palka, A.; Mencel, A.; Finster, J.; Mouscadet, J.-F.; Le Bret, M. *Lett. Drug Des. Disc.* **2006**, *3*, 175.
17. Polanski, J.; Niedbala, H.; Musiol, R.; Podeszwa, B.; Tabak, D.; Palka, A.; Mencel, A.; Mouscadet, J.-F.; Le Bret, M. *Lett. Drug Des. Disc.* **2007**, *4*, 99.
18. Musiol, R.; Tabak, D.; Niedbala, H.; Podeszwa, B.; Jampilek, J.; Kralova, K.; Dohnal, J.; Finster, J.; Mencel, A.; Polanski, J. *Bioorg. Med. Chem.* **2008**, *16*, 4490.
19. Musiol, R.; Jampilek, J.; Buchta, V.; Niedbala, H.; Podeszwa, B.; Palka, A.; Majerz-Maniecka, K.; Oleksyn, B.; Polanski, J. *Bioorg. Med. Chem.* **2006**, *14*, 3592.
20. Musiol, R.; Jampilek, J.; Kralova, K.; Richardson, D. R.; Kalinowski, D. S.; Podeszwa, B.; Finster, J.; Niedbala, H.; Palka, A.; Polanski, J. *Bioorg. Med. Chem.* **2007**, *15*, 1280.
21. Mekouar, K.; Mouscadet, J. F.; Desmaele, D.; Subra, F.; Leh, H.; Savoure, D.; Auclair, C.; d'Angelo, J. *J. Med. Chem.* **1998**, *41*, 2846.
22. Bonnenfant, S.; Thomas, C. M.; Vita, C.; Subra, F.; Deprez, E.; Zouhiri, F.; Desmaele, D.; d'Angelo, J.; Mouscadet, J. F.; Leh, H. *J. Virol.* **2004**, *78*, 5728.
23. Ma, X. H.; Zhang, X. Z.; Tan, J. J.; Chen, W. Z.; Wang, C. X. *Acta Pharmacol. Sin.* **2004**, *25*, 950.
24. Hare, S.; Gupta, S. S.; Valkov, E.; Engelman, A.; Cherepanov, P. *Nature* **2010**, *464*, 232.
25. Maertens, G. N.; Hare, S.; Cherepanov, P. *Nature* **2010**, *468*, 326.
26. Cherepanov, P. *EMBO Rep.* **2010**, *11*, 328.
27. Li, X.; Krishnan, L.; Cherepanov, P.; Engelman, A. *Virology* **2011** in press, doi:10.1016/j.virol.2010.12.008.
28. Hare, S.; Vos, A. M.; Clayton, R. F.; Thuring, J. W.; Cummings, M. D.; Cherepanov, P. *PNAS* **2010**, *107*, 20057.
29. Behforouz, M.; Haddad, J.; Cai, W.; Arnold, M. B.; Mohammadi, F.; Sousa, A. C.; Horn, M. A. *J. Org. Chem.* **1996**, *61*, 6552.
30. Altomare, A.; Cascarano, G.; Giacovazzo, C.; Guagliardi, A.; Moliterni, A.; Burla, M.; Polidori, G.; Camalli, M.; Spagna, R. *J. Appl. Crystallogr.* **1994**, *27*, 436.
31. Sheldrick, G. M. SHELXL97. Program For Crystal Structure Refinement, University of Göttingen, 1997.
32. Farrugia, L. J. *J. Appl. Crystallogr.* **1997**, *30*, 565.
33. Burgi, H.-B.; Dunitz, J. *Structure Correlation*; VCH, 1994.
34. Courcot, B.; Firley, D.; Fraisse, B.; Becker, P.; Gillet, J.-M.; Pattison, P.; Chernyshov, D.; Sghaier, M.; Zouhiri, F.; Desmaele, D.; d'Angelo, J.; Bonhomme, F.; Geiger, S.; Ghermani, N. E. *J. Phys. Chem. B* **2007**, *111*, 6042.
35. Zouhiri, F.; Mouscadet, J.-F.; Mekouar, K.; Desmaële, D.; Savouré, D.; Leh, H.; Subra, F.; Le Bret, M.; Auclair, C.; d'Angelo, J. *J. Med. Chem.* **2000**, *43*, 1533.
36. De Luca, L.; Pedretti, A.; Vistoli, G.; Letizia Barreca, M.; Villa, L.; Monforte, P.; Chimirri, A. *Biochem. Biophys. Res. Commun.* **2003**, *310*, 1083.
37. Li, H.; Robertson, A. D.; Jensen, J. H. *Proteins* **2005**, *61*, 704.
38. Edelsbrunner, H.; Facello, M.; Fu, R.; Liang, J. *Proceedings of the 28th Hawaii International Conference on Systems Science*. 1995, p 256.
39. Molecular Operating Environment (MOE 2008.10) CCG Inc. 1255 University St., Suite 1600, Montreal, Quebec, Canada H3B 3X3, http://www.chemcomp.com/.
40. Zentgraf, M.; Steuber, H.; Koch, C.; La Motta, C.; Sartini, S.; Sotriffer, C. A.; Klebe, G. *Angew. Chem. Int. Ed.* **2007**, *46*, 3575.
41. Polanski, J.; Zouhiri, F.; Jeanson, L.; Desmaele, D.; d'Angelo, J.; Mouscadet, J.; Gieleciak, R.; Gasteiger, J.; Le Bret, M. *J. Med. Chem.* **2002**, *45*, 4647.